A FODO RACETRACK RING DESIGN AND OPTIMIZATION FOR nuSTORM*

A. Liu†, A. Bross, D. Neuffer, Fermi National Accelerator Laboratory, Batavia, USA

Abstract

The nuSTORM decay ring is a compact racetrack storage ring with a circumference of ~480 m with large aperture (60 cm diameter) magnets. There are many challenges in the design. In order to incorporate the Orbit Combination Section (OCS) designed for injecting the pion beam into the ring, a dispersion suppressor is needed adjacent to the OCS. Concurrently, in order to maximize the number of useful muon decays, strong bending dipoles are needed in the arcs to minimize the arc length. These dipoles create strong chromatic effects, which need to be corrected by nonlinear sextupole elements in the ring. The goal of the nuSTORM ring is to accept a muon beam as large as one with 2 mm rad unnormalized full transverse admittance (6 times the RMS emittance), and a momentum spread within 3.8±10% GeV/c. In this paper, a FODO racetrack ring design and its optimization using sextupolar fields via both a Genetic Algorithm (GA) and a Simulated Annealing (SA) algorithm will be discussed.

INTRODUCTION

The goal of nuSTORM [1, 2] is to provide well-defined neutrino beams for precise measurements of neutrino cross-sections and oscillations. The schematic drawing of the nuSTORM facility is presented in Figure 1. A high-intensity proton beam is directed onto a target, producing a large spectrum of secondary pions. The forward pions are focused by a collection magnetic horn and inserted through a chicane into the straight section of the storage ring. Pion decay within the straight section produces muons which are within the circulating acceptance of the storage ring, where they are stored for approximately the muon lifetime [3]. Muons that decay within the production straight section produce neutrino beams of known flux and flavor ($\mu^+ \rightarrow e^+ + \bar{\nu}_\mu + \nu_e$ or $\mu^- \rightarrow e^- + \bar{\nu}_e + \nu_\mu$).

The critical design challenge is in storing the maximal number of muons. The nuSTORM solution is to design a large-acceptance storage ring (accepting a momentum spread of $\delta = dP/P_0 \approx \pm 10\%$ and a transverse geometric admittance $6\epsilon_{\perp,rms}$ of 2 mm rad) and to inject higher-momentum pions from a large-acceptance pion beamline (PBL) into the production straight section. The PBL uses stochastic injection to guide the pion beam that centers at 5 GeV/c into the 3.8 GeV/c decay ring [4–6]. In order to implement the stochastic injection, a special injection section, named Orbit Combination Section (OCS) was designed to combine the orbits of the 5 GeV/c reference pion and 3.8 GeV/c reference muon. The performance of the PBL design was investigated in G4Beamline [7]. Figure 2 shows the distribution of pions in the transverse phase space at the downstream face of the magnetic collection horn, and that of the muons at the end of the PBL. An ellipse showing the fitted 2 mm·rad acceptance aperture is displayed. An Iterative Gauss-Newton (IGN) fitting method was used to remove the fitting bias caused by particles with extra-large emittance. Based on the PBL design, the horn can be optimized to obtain a 15% increase in neutrino flux [8].

The design of an OCS type stochastic injection requires the dispersion D_x to be large at the injection point, so that the two separate orbits can be combined. However, a large D_x naturally enlarges the beam size, and is hence harmful to the transmission in the ring. Accordingly, directly next to the injection point, D_x needs to be at a much lower value. In fact, D_x should be suppressed anywhere except at the OCS or the OCS mirror. This needs strong dipoles and quadrupoles, which create large natural chromaticities. Moreover, even if the linear dispersion D_x may vanish under certain designs, higher order terms $D_x^{(n)}$, which are usually ignorable for a low δ beam, are still non-negligible and enlarge the beam size. While the second-order dispersion $D_x^{(2)}$ can be corrected by sextupoles, they also perturb higher-order terms $D_x^{(3)}$ and more. The major purpose of adding sextupoles is to suppress the natural chromaticity, but it also introduces nonlinear resonances and geometric aberrations. Sextupoles are usually placed where linear dispersion D_x is large. Whereas as for a decay ring, long dispersion-free straight sections are desired, and the ratio of straight to arc needs to be as large as possible. Therefore, putting sextupoles in the nuSTORM FODO ring is much constrained.

Consequently, an algorithm is needed to choose the best sextupole correction scheme to optimize the acceptance of the large muon beam, directly from multi-particle tracking, rather than trying to correct all the chromatic and geometric aberration terms. A Genetic Algorithm (GA) or a Simulated Annealing (SA), both of which are metaheuristic, can be applied for this purpose. In this paper, the linear optics design of the nuSTORM FODO ring and the sextupole correction are discussed.

LINEAR OPTICS DESIGN

The nuSTORM decay ring incorporates the Orbit Combination Section (OCS) designed to join the two reference orbits of 5 GeV/c π and 3.8 GeV/c μ together. The illustrative schematic drawing of the OCS and production straight section of the ring is shown in Figure 3. The injection happens at the leftmost of the figure, while the undecayed pions can

* Work supported by Fermilab, Operated by Fermi Research Alliance, LLC under Contract No. DE-AC02-07CH11359 with the United States Department of Energy.

† aoliu@fnal.gov

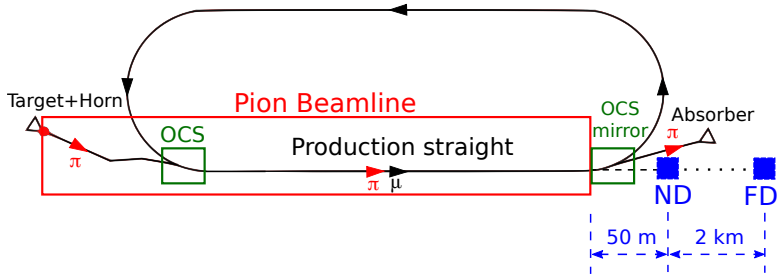

Figure 1: The schematic of the beamline structure in the nuSTORM facility

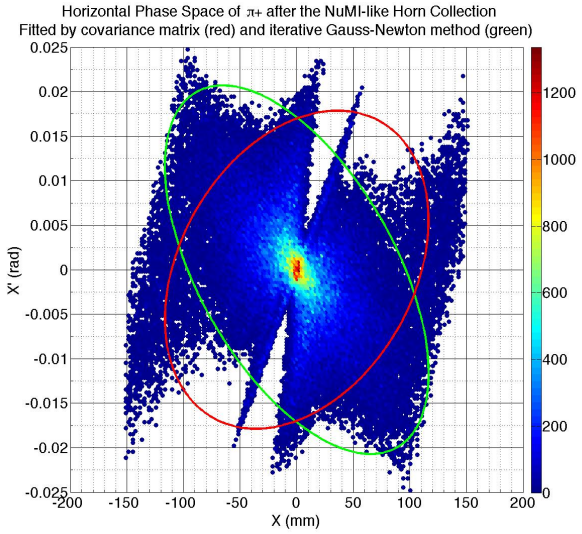

Figure 2: The distribution of 5 ± 1 GeV/c pions in the transverse phase space, as generated using MARS15 [9], and the corresponding fitted 2 μm·rad Gaussian acceptance ellipse. The fitting results from the IGN method and the covariance matrix are shown in green and red, respectively. The IGN method conserves the core shape of the distribution.

be extracted in the "mirror OCS" at the end of the production straight.

The production straight is composed of standard FODO cells, within which muons decay to useful neutrinos when passing. The FODO cells are designed to accommodate both muons and pions by providing separate periodic optics for the two reference momenta. The optics of the 3.8 GeV/c reference μ from the FODO cell to the injection point is shown in Figure 4, in which beams move from right to left. $D_x^{(0)}$ at the injection point was intentionally designed to be large to allow for a 40 cm separation from the two reference orbits at injection.

There are two schemes for the arc design. In the first scheme, the average linear dispersion is kept small by implementing the achromat cell structure. The other uses combined-function dipoles with nonzero $D_x^{(0)}$ in arcs. Large $\beta_\perp$ in the production straight FODO cells are preferred because of the small $\sigma_{x'}$ associated with them. Nevertheless, as for the non-production straight, which connects the other ends of the arcs, smaller $\beta_\perp$ are referable because of the beam size. $\beta_\perp$ in the non-production straight can also be adjusted to avoid resonance tunes. As a result, the ring has only one reflection symmetry, for which the reflection axis is the connection between the straight section centers.

The circumference of the ring is approximately 480 meters, which is slightly bigger than the Fermilab Booster. With arcs of approximately 60 meters as in the preferred design scheme being discussed later, the fraction of the ring circumference that is useful for neutrino production is ~ 0.39. This geometry also makes it possible to utilize the intense ν_μ or $\bar{\nu}_\mu$ beam from the injected π^+ or π^- decay, as the neutrino signals can be distinguished from electron and muon neutrinos from muon decay through timing.

With the above circumference the lifetime of 3.8 GeV/c muons in the lab frame, approximately 87% of them will decay in 100 turns. Consequently, the number of muons that survive 100 turns in tracking without decay is used as the "benchmark" for comparing the ring designs. In this section, two arc designs, one with superconducting combined function magnets and the other with separate function superconducting dipoles and normal-conducting quadrupoles, are presented.

Arc design with superconducting combined function magnets

In this design, superconducting combined-function magnets were used. The combined-function magnets have the advantage of making a compact arc, and reducing the natural chromaticity, C_x, which is given by

$$\frac{\beta_x}{4\pi}\oint\Big[-\frac{2}{\rho^2}+K+2\frac{D_x^{(1)}}{\rho}\left(\frac{1}{\rho^2}-K\right)-\left(\frac{1}{\rho}\right)' D_x^{(1)\prime}+\frac{\gamma_x}{\beta_x\rho}D_x^{(1)}\Big]ds$$

where the combined function magnets, with strong dipole field and therefore smaller bending radius, suppress C_x. The linear optics of this design is shown in Figure 5. The key parameters of the ring is shown in Table 1.

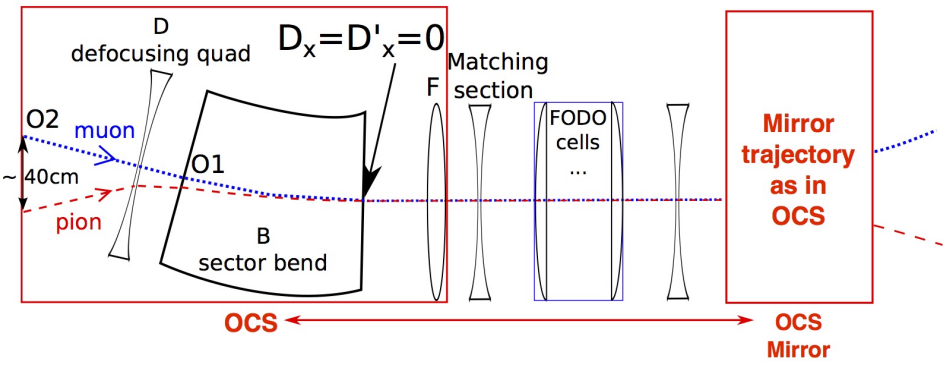

Figure 3: The schematic drawing of the OCS and production straight part of the decay ring.

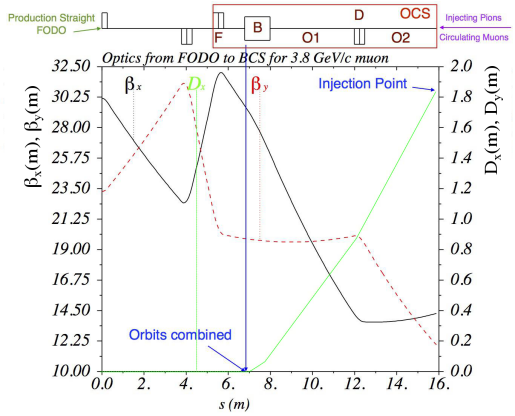

Figure 4: The 3.8 GeV/c reference μ optics from the FODO straight to the injection point. Both circulating muons and pions being injected travel from right to left.

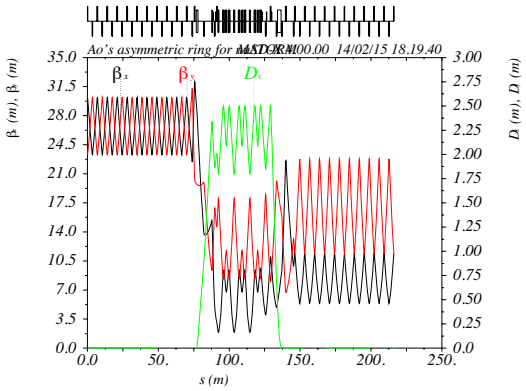

Figure 5: The Twiss functions of the ring design with arcs formed by superconducting combined-function magnets.

However, as written above, the natural linear chromaticity is only one of the many factors that determines the ring performance. In order to find the tune footprint of the ring lattice, a Frequency Map Analysis (FMA) method, analyzed by *elegant* [10], is employed to gain more insight, especially on the nonlinear properties of the ring. First the tune shifts with amplitude are checked with on-momentum particles.

Table 1: Parameters of the decay ring design with combined function dipole arcs

Parameters	Values (units)
Central momentum $P_{0,\mu}$	3.8 (GeV/c)
Circumference	488.5 (m)
Arc length	59.8 (m)
Production straight L	181.56 (m)
Non-production straight L	187.34 (m)
(ν_x, ν_y)	(8.12, 4.63)
$(d\nu_x/d\delta, d\nu_y/d\delta)$	(-4.11,-6.62)

The FMA of on-momentum particles with proper aperture limits added in *elegant* is shown in the upper plots of Figure 6. The lower plots show that the chromatic effects of this design are checked by doing the FMA analysis on particles with a full momentum range of $\delta \in \pm 10\%$.

As illustrated by the plots, the natural chromaticities are greatly reduced in this scenario, as in an ordinary FODO ring design the chromaticities are slightly larger than the betatron tunes of the ring. The tune dependence on the particle action is small for this design, however the chromatic driving terms still dilute the tune distribution in the tune plane without a clear pattern. Because of the combination of chromatic and geometric nonlinear effects in the ring, the FMA yielded a scattered accepted tunes on the tune plane. Thus the acceptance of the lattice needs to be determined by symplectic multi-particle tracking using MADX-PTC [11]. The tracking was done for a muon beam with Gaussian transverse distribution, for which the transverse admittance is 2000 μm·rad, and uniform momentum distribution within 3.8 ± 10% GeV/c. Without the sextupole correction, the number of particles surviving 100 turns is 58%, and around ~ 10% of the particles are lost within the first turn. More specifically, the loss is highest at the OCS, where both β_x and D_x are large. This big loss is to some extent inevitable because of the stochastic injection functionality of the OCS.

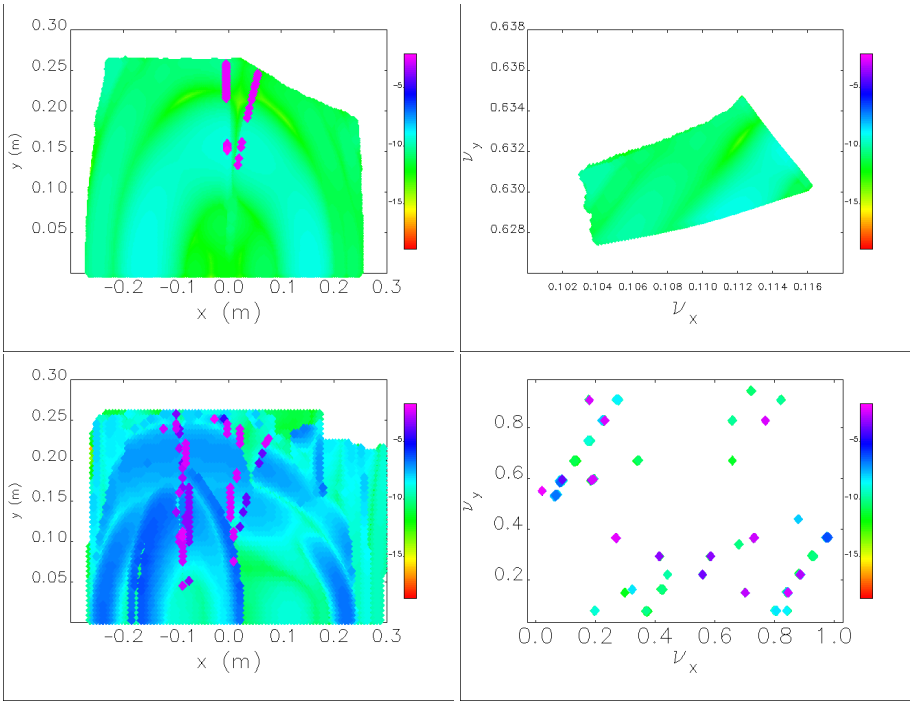

Figure 6: The Frequency Map Analysis (FMA) of the ring design with combined function dipoles in the arcs in the X-Y space (left) and on the betatron tune plane (right), on-momentum particles (upper) and off-momentum particles within the full range of $\delta = \pm 0.1$ (lower) are analyzed. No sextupole corrections added.

Arc design with normal-conducting combined function magnets

As a comparison, another possible design option was proposed to avoid the complexity of introducing cryogenic equipment into the facility. The idea of using combined function dipoles to reduce the natural The arc was redesigned to include only normal-conducting combined-function dipoles. The parameters of the new design option are listed in Table 2, and the linear optics are plotted in Figure 7.

Table 2: Parameters of the decay ring design with non-superconducting arc dipoles

Parameters	Values (units)
Circumference	535.9 (m)
Arc length	86.39 (m)
Straight length	181.56 (m)
(ν_x, ν_y)	(6.23, 7.21)
$(d\nu_x/d\delta, d\nu_y/d\delta)$	(-3.11,-12.73)

Compared that with superconducting dipoles in the arcs, the new design has a bigger circumference (536 compared to 488), and requires more combined function dipoles (24 compared to 13). The drift space between magnets is also too small for individuals sextupoles to be placed, therefore, the sextupole correction could be added only to the combined-function dipoles to make them multipoles, which still keeps the pole-tip field below 2 Tesla. The survival rate for 100 turns before sextupole corrections is 50%.

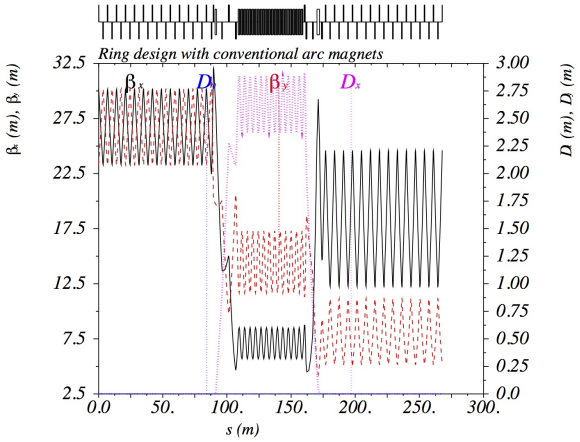

Figure 7: The linear optics of a nuSTORM decay ring design with conventional combined function dipoles in the arcs. β_x: black, β_y: red, D_x: purple.

SEXTUPOLE CORRECTION OPTIMIZATION USING A GENETIC ALGORITHM

Sextupole correction is needed in the ring to improve the acceptance of the ring. In this section, the correction scheme and its optimization for the first ring design with superconducting arc design are described.

Due to the space limits between magnets, sextupole fields also need to be added to the quadrupoles in the arcs to form

combined function multipoles, which are limited to have less than 4 Tesla pole-tip fields. The quadrupole-sextupole combined function magnets have been designed and tested by many experiments, for example in [12]. This allows 3 combined function multipoles and three individual sextupoles, all at dispersive locations, to carry sextupole fields. Using this method, the length of the arcs can be kept as short as possible.

The Genetic Algorithm has been applied in many accelerator fields, including muon facilities [8]. The algorithm is capable of testing a wide range in parameter space to propose new generations of individual solutions that have a high probability of surpassing the older generation. In this study, the same GA module as described in [8], written in Python, was used on NERSC. In this study, the single objective of the optimization is to increase the number of the particles that may survive 100 turns. The fitness value for this objective is the percentage of the initial muons that can survive 100 turns in multi-particle tracking computed by the MAD-X PTC_TRACK [13] module. The tracking is started from the middle of the production straight shown as the starting point in Figure 5. The initial muon beam is generated based on the covariance matrix of the beam at that point with the momentum of particles uniformly distributed within 3.8 ± 10% GeV/c, and the transverse phase space normally distributed within the 2 mm·rad admittance. After the optimization, the acceptance of the beam was increased to 67% from 58%.

The FMA of the post-optimization ring design are shown in Figure 8. The FMA results imply that the sextupole corrections are not capable of correcting all the higher order terms.

The histograms of the average survival turns for particles in each momentum bin are shown in Figure 9. Both the pre-optimization and post-optimization lattice tracking results are plotted and compared. It is observed that, there are major stopbands at two δ locations, $\delta \approx -0.05$ and $\delta \approx 0.03$. When $|\delta|$ is close to 0.1, the acceptance is further limited by higher-order chromatic effects, such as the terms in Table 3. The algorithm, while not able to correct all the nonlinear effects, finds the global optimum and nicely corrects one stopband.

Table 3: Comparison of the principal terms corrected by the sextupole optimization

Parameters	Before sextupole correction	After sextupole optimization
$d\nu_x/d\delta$	-4.29	-4.61
$d^2\nu_x/d\delta^2$	-3.62	0.41
$d^3\nu_x/d\delta^3$	-326	166
$d\nu_y/d\delta$	-7.34	-6.68
$d^2\nu_y/d\delta^2$	-10.7	-3.79
$d^3\nu_y/d\delta^3$	-94.1	-78.5
D_2	21.2	1.57
D_3	958	831

In order to validate the optimization and investigate on the $\delta \sim 0.03$ stopband shown in Figure 9 that the GA did not improve, a special test beam, with 2 mm·rad transverse admittance and $\delta \in [0.02, 0.04]$ was generated for tracking. The optimization was run again to find the optimum correction scheme specifically for this beam, which indicates whether it is possible for the previous optimizations to simultaneously correct this stopband. The acceptance for this beam was increased from only 16% to 88% by the algorithm. As a comparison, the average number of survived turns for particles in each momentum bin, corresponding to Figure 9, is plotted in Figure 10.

It can be seen that, the stopband at $\delta = 0.03$ was successfully corrected by the optimization. The comparison of this correction scheme and the optimized correction scheme is shown in Figure 11. The color of each marker represents the increase in the acceptance at each $\delta - \epsilon_{ad}$ value combination. The low acceptance of the full-sized beam (upper-right points) confirms that the correction of this momentum stopband creates other nonlinearities and thus is not a globally optimum configuration. The figure indicates that the globally optimized correction scheme works better when the momentum spread and transverse admittance of the beam is higher, while if the optimization is done locally, it works well only for a certain beam distribution.

CONCLUSIONS

The nuSTORM muon decay ring aims to accept a muon beam with both a large transverse admittance of 2000 μm and a large momentum range of 3.8±10% GeV/c. It has been shown that the beam is greatly affected by the nonlinearities of the lattice. Due to the constraints on the ratio of arc section lengths to straight section lengths, the sextupole correction for the nonlinearities is limited by the number of sextupoles or sextupolar fields that can be placed in the ring and their strengths. A design with arc cells formed by superconducting combined function dipoles was discussed in this paper. From a multi-particle tracking simulation in MAD-X, in which the beam was normally distributed in the 2 mm·rad admittance and uniformly distributed in 3.8 ± 10% GeV/c, 58% of the particles survive after circulating by 100 turns. The sextupole correction scheme was optimized with a genetic algorithm, the acceptance of the designs is increased to 67%. The effectiveness of the optimization was validated by using different initial beams and optimizations. It was shown that the heuristic algorithms can find the best balance among all the dominant nonlinearities for each beam, and find the global optimum of the problem.

ACKNOWLEDGMENT

The authors thank Dr. Mark Palmer for his supports on nuSTORM, Dr. David Adey for the discussions on the neutrino physics, and the MAP program colleagues on the discussions about the design. This research used resources of the National Energy Research Scientific Computing Center, a DOE Office of Science User Facility supported by the

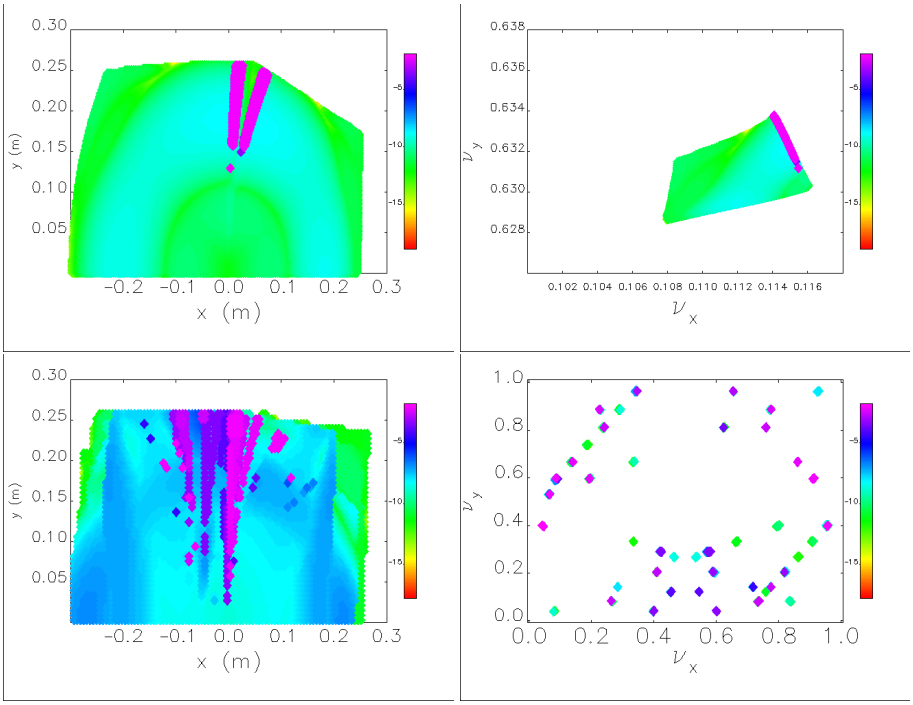

Figure 8: The FMA of the post-sextupole optimization ring design with combined function dipoles in the arcs in the X-Y space (left) and on the betatron tune plane (right), on-momentum particles (upper) and off-momentum particles within the full range of $\delta = \pm 0.1$ (lower) are analyzed.

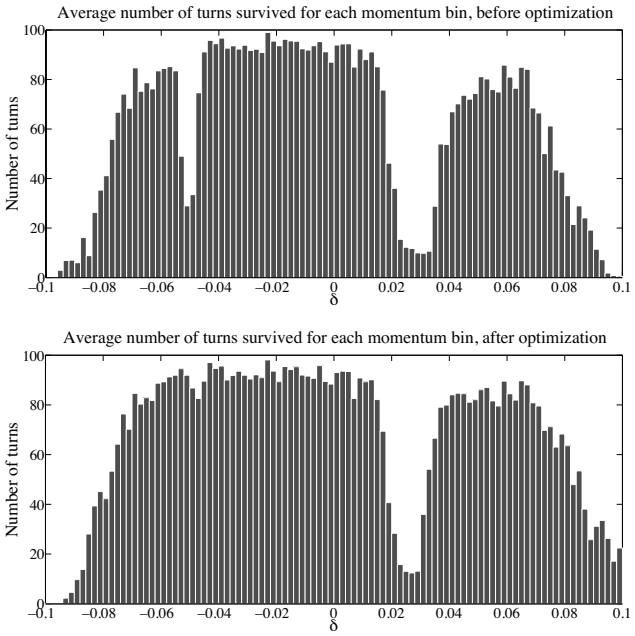

Figure 9: The average number of turns that particles in each momentum bin survive. The initial beam has a 2 mm·rad transverse admittance and a momentum spread of $\delta \in \pm 10‰$. The upper and lower plots correspond to data from the pre-optimized lattice and post-optimized lattice

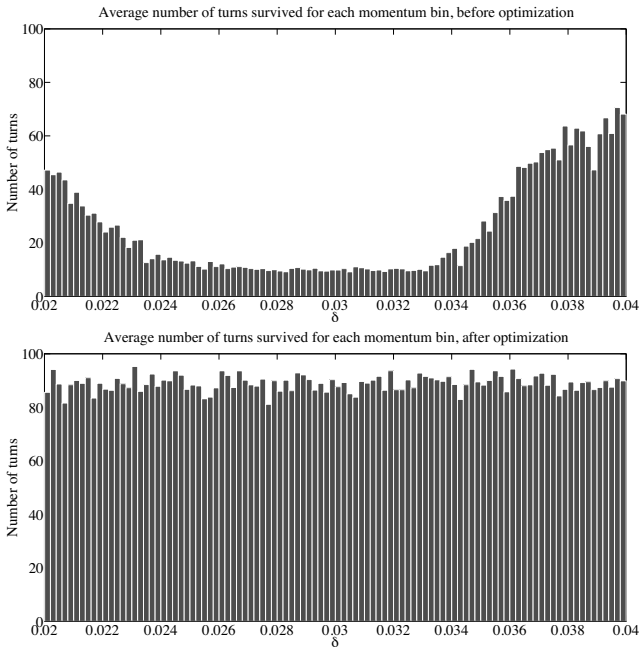

Figure 10: The average number of turns that particles in each momentum bin survive. The data were obtained from tracking of 10^5 particles, with 2 mm·rad transverse emittance and a momentum spread of $\delta \in [0.02, 0.04]$. The upper and lower plots correspond to data from the pre-optimized and post-optimized lattice.

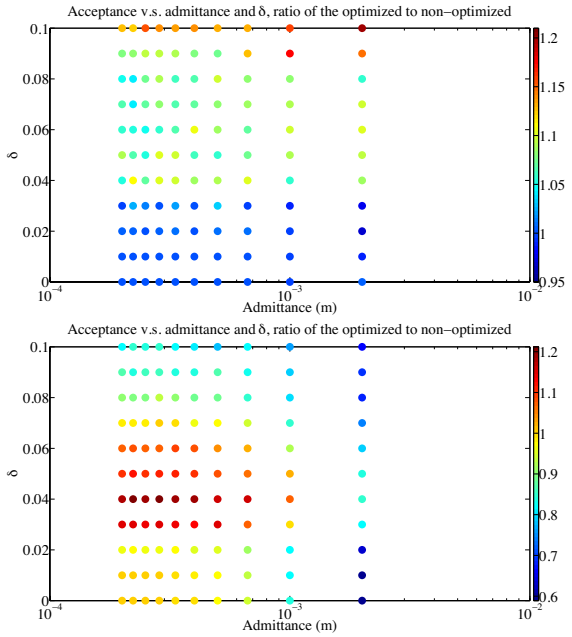

Figure 11: The increase in acceptance of different beams, represented by the ratio of the acceptance of the optimized lattices to the linear lattice. Upper: the original optimized lattice; Lower: the optimized lattice for a beam with 2 mm·rad transverse admittance and a momentum spread of $\delta \in [0.02, 0.04]$.

Office of Science of the U.S. Department of Energy under Contract No. DE-AC02-05CH11231.

REFERENCES

[1] P. Kyberd *et al.*, "nuSTORM - Neutrinos from STORed Muons: Letter of Intent to the Fermilab Physics Advisory Committee," 2012.

[2] D. Adey *et al.*, "Light sterile neutrino sensitivity at the nustorm facility," *Phys. Rev. D*, vol. 89, p. 071301, Apr 2014.

[3] D. Neuffer, "Design considerations for a muon storage ring," 1980. Telmark Conference on Neutrino Mass, Barger and Cline eds., Telmark, Wisconsin.

[4] D. Neuffer and A. Liu, "Stochastic injection scenarios and performance for nustorm," *Proc. IPAC2013, Shanghai, China, TUPFI055*, p. 1469, 2013.

[5] A. Liu, A. Bross, D. Neuffer, and S. Lee, "ν storm facility design and simulation," 2013.

[6] A. Liu *et al.*, "Design and simulation of the nustorm pion beamline," *Nuclear Instruments and Methods in Physics Research Section A*, vol. 801, pp. 44–50, 2015.

[7] T. Robert, "G4beamline main website." `http://http://www.muonsinternal.com/muons3/G4beamline`.

[8] A. Liu *et al.*, "Optimization of the magnetic horn for the nustorm non-conventional neutrino beam using the genetic algorithm," *Nuclear Instruments and Methods in Physics Research Section A*, vol. 794, pp. 200–205, 2015.

[9] N. Mokhov, "Mars15, website link http://www-ap.fnal.gov/mars/intro_manual.html."

[10] M. Borland, "Advanced photon source, anl." `http://www.aps.anl.gov/Accelerator_Systems_Division/Accelerator_Operations_Physics/software.shtml#elegant`.

[11] F. Schmidt, "Mad-x ptc integration," in *Particle Accelerator Conference, 2005. PAC 2005. Proceedings of the*, pp. 1272–1274, May 2005.

[12] W. Beeckman *et al.*, "Design, fabrication, measurement, installation and alignment of 2 types of quadrupole-sextupole combined magnets for the upgrade of the 1.2 gev booster synchrotron at tohoku university," in *Proceedings of the Particle Accelerator Conference, 2013. PAC 2013.*, pp. 1229–1231, 2013.

[13] L. Deniau *et al.*, "Mad project main web page." `http://mad.web.cern.ch/mad/`, 2002-Now.